ACS Infectious Diseases

Article

Cite This: ACS Infect. Dis. XXXX, XXX, XXX−XXX

pubs.acs.org/journal/aidcbc

Antischistosomal Properties of Sclareol and Its Heck-Coupled Derivatives: Design, Synthesis, Biological Evaluation, and Untargeted Metabolomics

Alessandra Crusco,[†,‡] Helen Whiteland,[†] Rafael Baptista,[†] Josephine E. Forde-Thomas,[†] Manfred Beckmann,[†] Luis A. J. Mur,[†] Robert J. Nash,[§] Andrew D. Westwell,[*,‡] and Karl F. Hoffmann[*,†]

[†]Institute of Biological, Environmental and Rural Sciences (IBERS), Aberystwyth University, Penglais Campus, Aberystwyth SY23 3DA, United Kingdom

[‡]School of Pharmacy and Pharmaceutical Sciences, Cardiff University, Cardiff CF10 3NB, United Kingdom

[§]PhytoQuest Limited, Plas Gogerddan, Aberystwyth, Ceredigion SY23 3EB, Wales, United Kingdom

Supporting Information

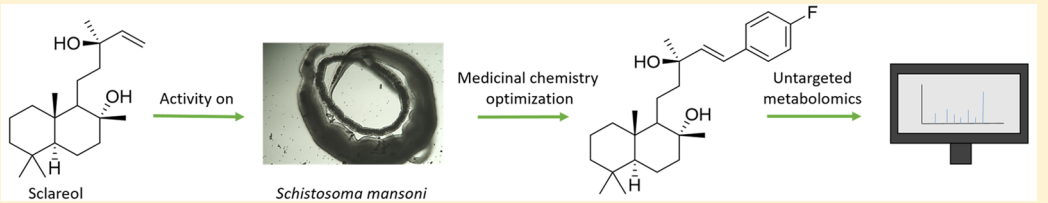

ABSTRACT: Sclareol, a plant-derived diterpenoid widely used as a fragrance and flavoring substance, is well-known for its promising antimicrobial and anticancer properties. However, its activity on helminth parasites has not been previously reported. Here, we show that sclareol is active against larval ($IC_{50} \approx 13\ \mu M$), juvenile ($IC_{50} = 5.0\ \mu M$), and adult ($IC_{50} = 19.3\ \mu M$) stages of *Schistosoma mansoni*, a parasitic trematode responsible for the neglected tropical disease schistosomiasis. Microwave-assisted synthesis of Heck-coupled derivatives improved activity, with the substituents choice guided by the Matsy decision tree. The most active derivative **12** showed improved potency and selectivity on larval ($IC_{50} \approx 2.2\ \mu M$, selectivity index (SI) ≈ 22 in comparison to HepG2 cells), juvenile ($IC_{50} = 1.7\ \mu M$, SI = 28.8), and adult schistosomes ($IC_{50} = 9.4\ \mu M$, SI = 5.2). Scanning electron microscopy studies revealed that compound **12** induced blebbing of the adult worm surface at sublethal concentration (12.5 μM); moreover, the compound inhibited egg production at the lowest concentration tested (3.13 μM). The observed phenotype and data obtained by untargeted metabolomics suggested that compound **12** affects membrane lipid homeostasis by interfering with arachidonic acid metabolism. The same methodology applied to praziquantel (PZQ)-treated worms revealed sugar metabolism alterations that could be ascribed to the previously reported action of PZQ on serotonin signaling and/or effects on glycolysis. Importantly, our data suggest that compound **12** and PZQ exert different antischistosomal activities. More studies will be necessary to confirm the generated hypothesis and to progress the development of more potent antischistosomal sclareol derivatives.

KEYWORDS: *diterpenoids, schistosomiasis, anthelmintic, sclareol, microwave synthesis, untargeted metabolomics*

Sclareol is a labdane diterpenoid widely used as a fragrance[1] as well as a food flavoring substance[2] and is generally considered safe for topical and oral administration.[3] Originally isolated from *Salvia sclarea*, sclareol is also found in essential oils derived from other *Salvia* spp which are thought to be produced in response to infection by bacteria and fungi.[4] These plant-defense properties have led to further mechanistic investigations, which have demonstrated sclareol's potency as an antibacterial,[5] antifungal,[6] and anticancer agent.[7−10] However, to the best of our knowledge, the activity of sclareol against parasitic helminths has not been previously investigated. As part of our ongoing efforts in identifying and characterizing anthelmintic phytochemicals, we now report the activity of sclareol and new synthetic analogues against the causative helminth responsible for schistosomiasis.

Schistosomiasis is a chronic, debilitating helminthiasis caused by parasitic trematodes within the genus *Schistosoma* and currently affects approximately 600 million people.[11] This disease is predominantly found in tropical areas of the world and, with up to 300,000 deaths per year, is considered the most deadly neglected tropical disease (NTD).[12] In the absence of a prophylactic vaccine, schistosomiasis is primarily controlled by a single drug, praziquantel (PZQ). This pyrazino-isoquinolone is active against the adult stages of all human-infective

Received: January 28, 2019
Published: May 13, 2019

DOI: 10.1021/acsinfecdis.9b00034
ACS Infect. Dis. XXXX, XXX, XXX−XXX

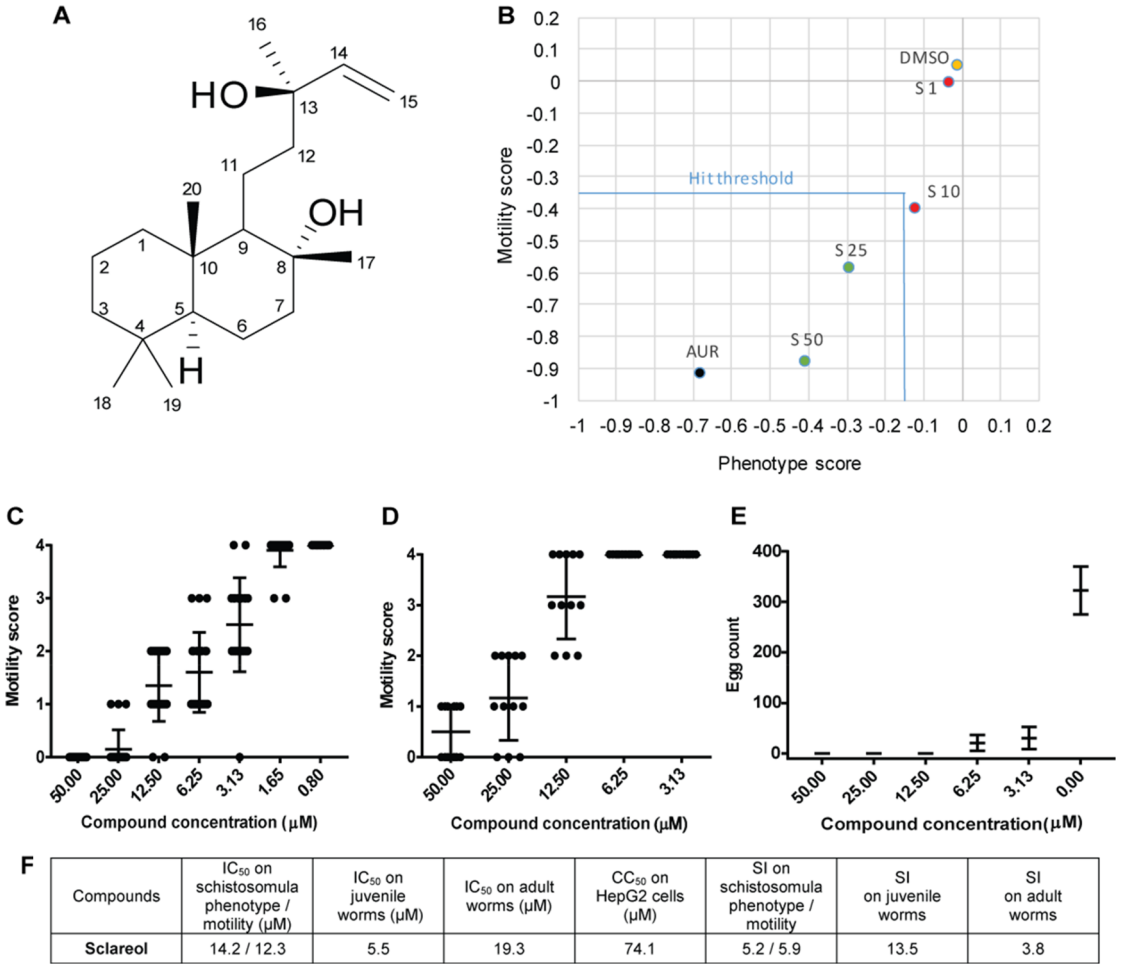

F

Compounds	IC_{50} on schistosomula phenotype / motility (μM)	IC_{50} on juvenile worms (μM)	IC_{50} on adult worms (μM)	CC_{50} on HepG2 cells (μM)	SI on schistosomula phenotype / motility	SI on juvenile worms	SI on adult worms
Sclareol	14.2 / 12.3	5.5	19.3	74.1	5.2 / 5.9	13.5	3.8

Figure 1. Structure and antischistosomal activity of (−)-sclareol. (A) Structure and scaffold numbering system of the diterpenoid (−)-sclareol. (B) Sclareol affects the phenotype and motility of *S. mansoni* schistosomula in a dose-dependent manner (50−1 μM). Schistosomula cocultivated with negative (0.625% DMSO) and positive (Auranofin 10 μM, 0.625% DMSO) controls are also indicated. The screening was performed by the high throughput screening platform Roboworm[18,27] with each point being the average of two replicates (each replicate contains 120 parasites/well). Hit compounds (within the hit threshold) affect ≥70% of the larvae. Z′-scores:[28] 0.69 for phenotype and 0.48 for motility. (C) Sclareol affects the motility of mixed-sex *S. mansoni* juvenile worms in a dose-dependent manner (50−0.8 μM) and of (D) mixed-sex *S. mansoni* adult worms (50−3.13 μM). Scores were calculated according to the Methods. Each point represents a single worm (10 juveniles × 2 independent experiments, 3 worm pairs × 2 independent experiments) with mean ± SD illustrated. (E) Sclareol inhibits egg production of *S. mansoni* adult worm couples when compared to control treatment (0.00). Values are mean ± SD of egg counts from 3 worm pairs × 2 independent experiments. (F) Estimated IC_{50}'s (μM) calculated from dose response curves on schistosomula phenotype and motility and on juvenile and adult worm motility, estimated CC_{50} on HepG2 human liver cell and selectivity index (SI).

Schistosoma spp but not on immature forms and, therefore, requires repeat administrations to maximize efficacy.[13] Furthermore, the fear of selecting for PZQ insensitive or resistant parasites drives the need to identify new anti-schistosomal drugs with a different mechanism of action to PZQ. The identification of such compounds will contribute to the sustainable control of schistosomiasis into the future.[14]

Toward this end, several diterpenoids with antischistosomal activity have been previously reported,[15−17] including several from our group.[18,19] The collective results of these investigations demonstrate that this molecule class could be a promising source of next generation anthelmintic. In this study, the antischistosomal activity of sclareol was demonstrated on larval, juvenile, and adult stages of *Schistosoma mansoni*, and this activity was considerably improved by the creation and testing of semisynthetic derivatives. On the basis of initial structural-activity relationships (SARs) derived from a first group of analogues, different Heck-coupled derivatives were synthesized on the basis of a previously reported synthetic route[20] and significantly improved by microwave-assisted synthesis. The choice of substituents was guided by the Matsy decision tree,[21] an updated version of the more classical Topliss scheme.[22] This process led to the synthesis of the most active compound **12** (IC_{50} ≈ 2.2 μM for schistosome larvae, selectivity index (SI) > 20 in comparison to HepG2 cells; IC_{50} = 1.7 μM for juveniles, SI = 28.8; IC_{50} = 9.4 μM for schistosome adults, SI = 5.2). The effects of compound **12** on schistosome phenotype were investigated by scanning electron microscopy (SEM), revealing tegumental alterations at a sublethal dose, characterized by swelling and bubble-like protrusions. Untargeted metabolomics of treated adult worms revealed significant alterations in lipid balance and, in particular, arachidonic acid (ARA) metabolism. These results are consistent with the previously reported effects of ARA on schistosome surface membranes.[23] Furthermore, the effect of compound **12** on schistosome metabolism is quite distinct

DOI: 10.1021/acsinfecdis.9b00034
ACS Infect. Dis. XXXX, XXX, XXX−XXX

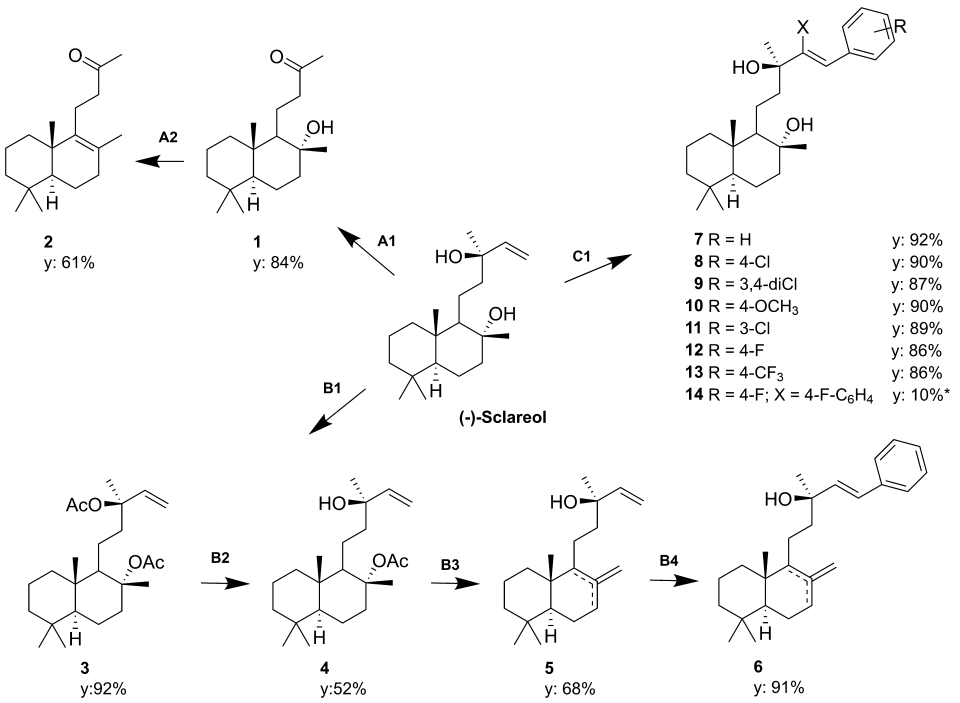

Figure 2. Derivatives of sclareol. Structures and synthetic scheme of the sclareol derivatives. When not specified, X = H.

from that induced by PZQ where alteration of sugar metabolism was predominantly observed. This metabolomics profile adds mechanistic support to the activity of PZQ in modulating serotonin signaling[24,25] and/or glycolysis[25,26] in schistosomes. The overall results of sclareol derivative synthesis, bioactivities, and the mechanism of action investigations (distinct from PZQ) are presented and discussed here.

RESULTS AND DISCUSSION

Anthelmintic Activity of (−)-Sclareol. The activity of a small collection of plant-derived diterpenoids (see Supporting Information, S1) on *S. mansoni* schistosomula (larvae), using the high throughput screening platform Roboworm,[18,27] identified anthelmintic properties among labdane-type diterpenoids. On the basis of this finding, we decided to ascertain the anthelmintic activity of enantiopure (−)-sclareol (Figure 1), the commercially available labdane diterpenoid (Figure 1A) more structurally related to the labdane hits in Supporting Information S1 (same condensed rings, open chain, and allylic alcohol group) and widely used in the cosmetic[1] and food[2] industries due to its excellent safety profile. Indeed, *in vivo* toxicity studies in mice have demonstrated a LD_{50} > 5000 mg/kg for both topical and oral delivery routes and a LD_{50} = 1000 mg/kg for the parental route.[3] Moreover, as sclareol is also well-known for its promising antimicrobial and antifungal activities,[5,6] we postulated that this labdane diterpenoid possessed biological properties (low toxicity and anti-infective nature) to warrant anthelmintic investigations. Therefore, sclareol's ability to affect motility and the phenotype of *S. mansoni* schistosomula was first assessed (final concentrations of 50−1 μM) by the Roboworm platform[18,27] (Figure 1B). Here, this diterpenoid demonstrated a dose-dependent antischistosomal activity with an IC_{50} of 14.2 μM for phenotype and 12.3 μM for motility (Figure 1B,F). Sclareol was then screened against juvenile (final concentrations of 50−0.8 μM) and adult worms (final concentrations of 50−3.13 μM) where it negatively affected worm motility (IC_{50} of 5.0 and 19.3 μM, respectively) (Figure 1C,D,F) and inhibited production of the pathogenic eggs at the lowest concentration tested (Figure 1E). We additionally confirmed the low toxicity of sclareol[3] on human HepG2 cells (CC_{50} = 74.1 μM) (Figure 1F). Considering the relative low toxicity of sclareol, we decided to pursue further medicinal chemistry studies on this diterpenoid to improve its anthelmintic characteristics.

Synthesis of Sclareol Derivatives. To quantify structural activity relationships and improve upon the moderate anthelmintic activity of sclareol, a small group of analogues was first synthesized (Figure 2). Oxidation of sclareol with $KMnO_4$ and $MgSO_4$ in acetone[29] led to the synthesis of compound **1**, with the allylic alcohol substituted by a keto group. Dehydration of compound **1** with I_2 in toluene[29] led to compound **2**. A further derivative of sclareol was obtained by acetylation of both alcoholic functions by acetyl chloride in the presence of *N*,*N*-dimethylaniline in dichloromethane,[30] giving compound **3**, and subsequent selective hydrolysis by KOH in ethanol[30] leading to compound **4**. The latter was subjected to an E1 elimination by using $NaHCO_3$ in DMSO, as described by Rogachev et al.,[30] with some modifications using microwave conditions (200 °C, 100 W, 11 min); this procedure led to the synthesis of compound **5** as a geometric isomeric mixture (2:1 exo/endo isomer mixture, as determined by ^{1}H NMR integration; see Supporting Information, S2). The obtained dehydrated derivative was subjected to the Heck-reaction,[20] with yields and reaction times improved by microwave conditions (130 °C, 300 W, 12 min), leading to compound **6**. The same Heck-reaction was performed directly on sclareol, obtaining the direct derivative compound **7**.

To investigate the impact of these changes on anthelmintic activity, this first small set of compounds (**1**−**7**) was screened against the schistosomula stage of *S. mansoni*. Compounds **1** and **2** lost their potency (Table 1), showing that the allylic

DOI: 10.1021/acsinfecdis.9b00034
ACS Infect. Dis. XXXX, XXX, XXX−XXX

Table 1. Antischistosomal and HepG2 Cytotoxicity Activities[a]

compounds	IC_{50} on schistosomula phenotype/motility (μM)	IC_{50} on juvenile worms (μM)	IC_{50} on adult worms (μM)	CC_{50} on HepG2 cells (μM)	SI on schistosomula phenotype/motility	SI on juvenile worms	SI on adult worms
sclareol	14.2/12.3	5.5	19.3	74.1	5.2/5.9	13.5	3.8
1	>25	NA	NA	>100	NA	NA	NA
2	>25	NA	NA	>100	NA	NA	NA
3	>25	NA	NA	>100	NA	NA	NA
4	11.6/12.1	NA	NA	>100	NA	NA	NA
5	12.9/10.4	NA	NA	85.1	6.6/8.2	NA	NA
6	>25	NA	NA	74.1	NA	NA	NA
7	5.7/5.3	2.0	18.6	43.7	7.7/8.2	21.9	2.3
8	3.5/3.6	6.5	12.7	42.7	12.2/11.9	6.7	3.4
9	27.6/10.6	NA	NA	93.3	3.4/8.8	NA	NA
10[b]	>25	NA	NA	>100	NA	NA	NA
11	8.2/5.4	11.2	27.7	53.7	6.5/9.9	4.8	1.9
12	2.1/2.3	1.7	9.4	49.0	23.3/21.3	28.8	5.2
13	26.0/19.8	NA	NA	63.1	2.4/3.2	NA	NA
14	1.4/1.3	6.3	16.4	42.7	30.5/32.8	6.8	2.6

[a]Estimated IC_{50}'s (μM) calculated from dose response curves for *S. mansoni* schistosomula phenotype/motility and *S. mansoni* adult and juvenile worm motility. Estimated CC_{50}'s (μM) calculated from dose response curves for HepG2 cells and selectivity indices (SI) of the anthelmintic activity when compared to the cell line. The values are mean results of experiments in duplicate for helminths or triplicate for cells (IC_{50}'s and CC_{50}'s with 95% confidence intervals in Supporting Information, S3). [b]Solubility problem.

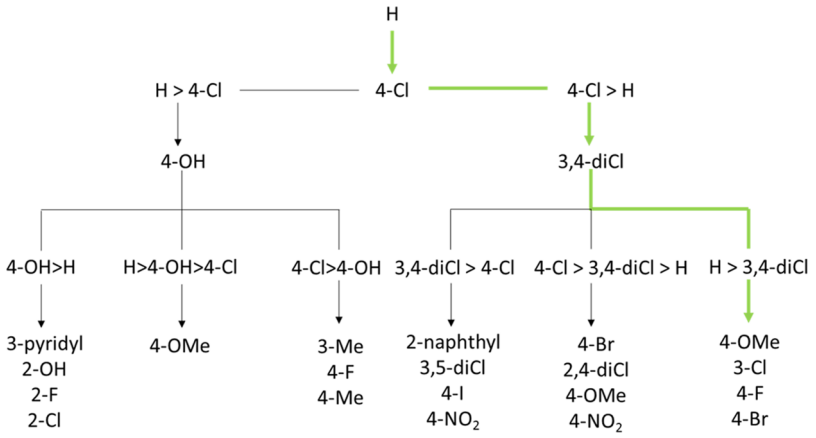

Figure 3. Matsy decision tree and pathway followed to generate more active antischistosomal compounds. The figure shows the Matsy decision tree by O'Boyle et al.,[21] an updated version of the classic Topliss decision tree. According to the increased or decreased activity brought by the different aromatic substituents, a pathway is followed leading to the choice of new substituents. The pathway followed in this study is highlighted in green. Adapted from ref 21. Copyright 2014 American Chemical Society.

portion is important for anthelmintic activity. The *bis*-acetylated compound **3** was inactive too, while the monoacetylated compound **4** recovered activity, comparable to sclareol, showing again that the free allylic alcohol is essential. The importance of the allylic alcohol for activity was also confirmed by comparison with the previous diterpenoid collection screening results (see Supporting Information, S1), where the two hit compounds **S6** and **S8** share this feature, while similar compounds presenting an inverted allylic alcohol (**S2**, **S10**) or replacement of the function (**S3**, **S9**) were not active. Compound **5** showed comparable activity to compound **4** (and to its plant-derived reference **S6**), while the addition of a phenyl ring in position 15 led to the loss of activity in compound **6**. Interestingly, this did not happen when the addition was made directly on sclareol to obtain compound **7**, which showed an almost 3-fold improved activity ($IC_{50} \approx 5.5$ μM) over sclareol. Thus, we decided to pursue the synthesis of new Heck-coupled derivatives (compounds **7**−**13**) with different phenyl substituents. The previous described synthesis route,[20] using $Pd(OAc)_2$, $Cu(OAc)_2$, and NaOAc in DMF at 80 °C, was followed and improved by microwave heating at 130 °C, leading to improved yields (from ∼60% to ∼90%) and improved reaction times (from 3−6 h to 11 min). Under microwave conditions, monocoupled products (**7**−**13**) with *trans* configuration, as shown by the ^{1}H NMR coupling constants of the alkene ($J \approx 16$ Hz), were obtained; when using classic thermal synthesis, Heck-coupling led to the *bis*-arylated products (**14**) in addition to monocoupled product (**12**).

To maximize the chance of finding more potent analogues against schistosomula while reducing the number of synthesis steps, the Matsy decision tree,[21] an updated version of the classical Topliss tree,[22] was followed (Figure 3). The first phenyl ring substitution with chlorine in the 4-position (compound **8**) improved the antischistosomula activity of compound **7** to an $IC_{50} \approx 3.5$ μM. The 3,4-dichloro-substituted compound **9** was then synthesized as suggested by the Matsy tree, but this led to decreased activity.

DOI: 10.1021/acsinfecdis.9b00034
ACS Infect. Dis. XXXX, XXX, XXX−XXX

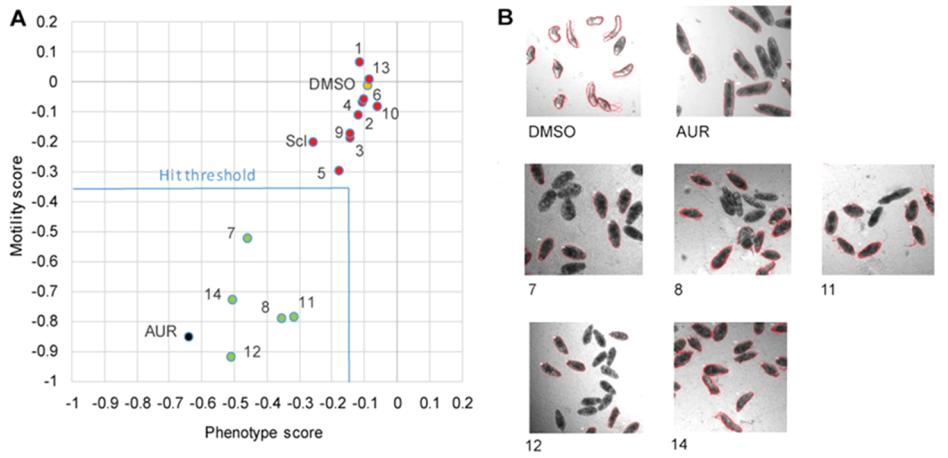

Figure 4. Screening of sclareol derivatives on *S. mansoni* schistosomula at 10 μM. (A) The synthesized derivatives (at 10 μM) were assessed for their ability to affect phenotype and motility of *S. mansoni* schistosomula when compared to the original sclareol (Scl, 10 μM) as well as to the negative (0.625% DMSO) and positive (Auranofin 10 μM, 0.625% DMSO) controls. The screening was performed by the high throughput platform Roboworm as previously described.[18] Hit compounds (within the hit threshold) affect ≥70% of the larvae. Each point represents the average score of two replicates. Z′-scores:[28] 0.41 for phenotype and 0.23 for motility. (B) Images of the parasites after treatment with the controls and the five hits at 10 μM are also shown. Control schistosomula presented a normal phenotype and high motility (indicated by change in red outlines), while affected schistosomula presented an altered phenotype (change in shape and darkening) and low or absent motility (no change in red outlines).

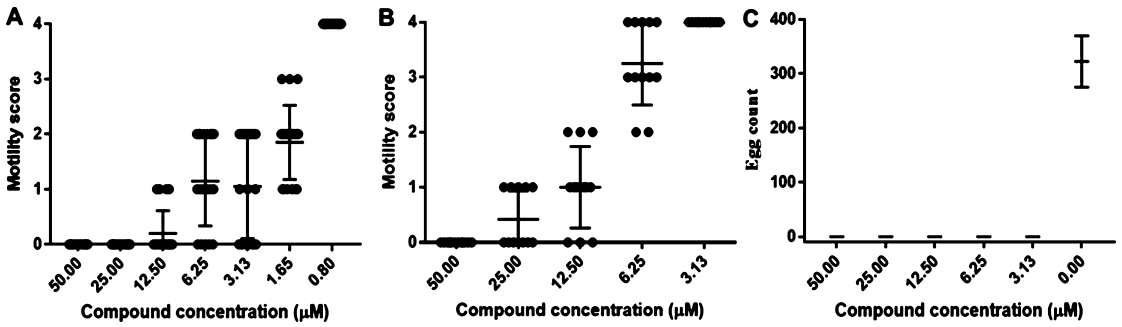

Figure 5. Screening of compound **12** on *S. mansoni* juvenile and adult worms. Compound **12** affects the motility of (A) *S. mansoni* juvenile worms (50−0.8 μM) and (B) *S. mansoni* adult worms (50−3.13 μM). Scores were calculated according to the Methods. Each point represents a single worm (10 juveniles × 2 independent experiments, 3 worm pairs × 2 independent experiments) with mean ± SD shown. (C) Compound **12** inhibits egg production (3 worm pairs/well × 2 replicate experiments) until the lowest concentration tested (3.13 μM) when compared to the DMSO control (0).

Subsequently, the far right branch of the tree was followed, leading to the synthesis of 4-OMe (compound **10**) and 3-Cl (compound **11**) substituted analogues (the first with a solubility problem, the second with lower activity) as well as a 4-F analogue (compound **12**), which showed the most potent activity (IC_{50} ≈ 2.2 μM, 6-fold more potent than sclareol). Taking into account the increased activity brought by the fluorine group, a 4-CF_3 derivative was also synthesized (compound **13**); the double addition side product generated from the classical reaction of compound **12** (compound **14**) was also tested. While compound **13** was less potent, the activity of the side product (compound **14**) was more potent (IC_{50} ≈ 1.3 μM). The greater antischistosomula activity associated with the double addition side product **14** could be correlated with increased lipophilia compared to the correspondent single addition product **12**, which in turn is more lipophilic and potent when compared to sclareol lacking a phenyl ring (calculated logP 7.9 > 6.4 > 4.7, respectively). Indeed, increased lipophilia could be responsible for a greater passage of the compound through the schistosomula membrane and, therefore, for better activity. However, changes in lipophilia brought about by phenyl substituents did not always follow this correlation (e.g., **8** is more potent than **9**, although calculated logP values are 6.8 and 7.4, respectively) and suggest that other factors likely contribute. However, when compounds were tested on juvenile and adult worms, as fully described in the next paragraph, compound **12** was the most potent.

Anthelmintic and Cytotoxic Screening of Derivatives. As described above, to help inform the progression of hit compound identification, compounds were first titrated (50 to 1 μM) on *S. mansoni* schistosomula by using the automated platform Roboworm, which scores parasites on the basis of their phenotype and motility.[18] A follow-up secondary screen of all synthesized compounds was subsequently completed to validate these results and to compare antischistosomal potency at 10 μM (Figure 4). In addition to this, all compounds were assessed for overt cytotoxicity by screening against the human HepG2 liver cell line (collective results shown in Table 1).

Compounds with IC_{50} values on schistosomula below 10 μM (**7**, **8**, **11**, **12**, and **14**) were then selected for follow-up experiments against juvenile and adult schistosomes (Table 1;

DOI: 10.1021/acsinfecdis.9b00034
ACS Infect. Dis. XXXX, XXX, XXX−XXX

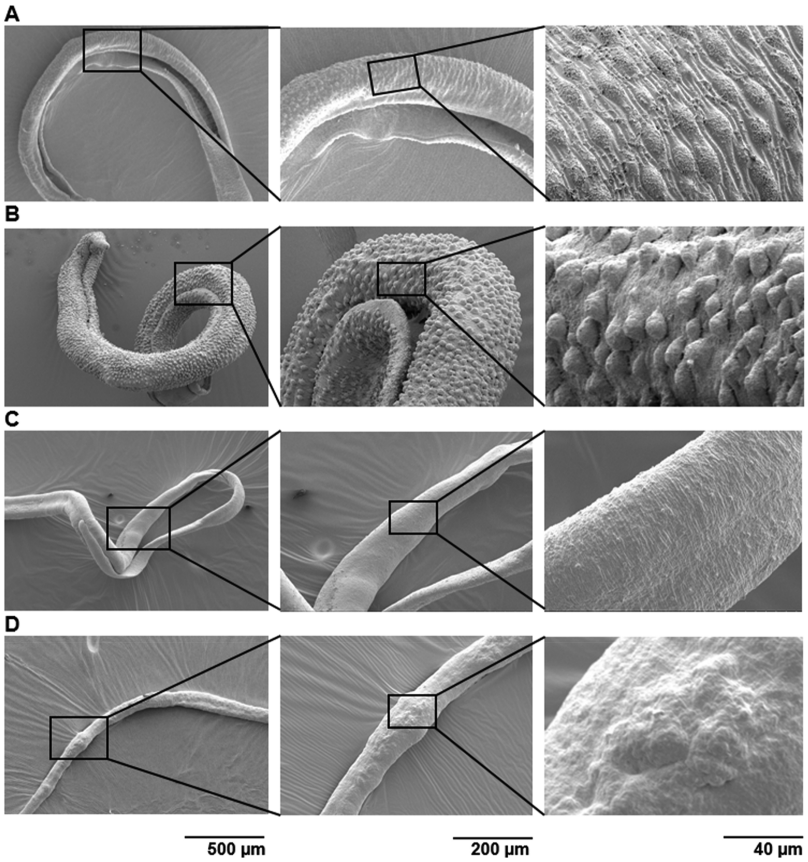

Figure 6. Scanning electron microscopy (SEM) images of *S. mansoni* worms cocultivated with compound **12**. SEM images of untreated adult male (A) and female (C) worms compared to male (B) and female (D) worms treated with compound **12** at 12.5 μM. The surface of the treated parasite appears damaged when compared to the control, and the presence of bubble-like protrusions and swelling is evident.

Supporting Information, S4 and S5). Similar to the antischistosomula screens, compound **12** showed the greatest activity (IC_{50} of 1.7 μM on juveniles, 9.4 μM on adults; Table 1) and inhibited egg production (despite worm recovery) at all concentrations tested (Figure 5).

Phenotypes of adult worms treated with a sublethal concentration (12.5 μM) of compound **12** were analyzed by SEM (Figure 6). The surface of treated parasites was altered when compared to the DMSO control and, in particular, blebbing, swelling of the tegument, and bubble-like protrusions were observed on both male and female worms (Figure 6A,C compared to Figure 6B,D). This suggested that the antischistosomal activity of compound **12** could be related to membrane or tegumental disruptions, as previously reported for other terpenoids.[16,17,31]

Untargeted Metabolomics. To further investigate the mode of action of compound **12**, analysis of metabolomic changes induced in adult worms cocultured at its IC_{50} value was performed as described in the Methods, adapting the procedure applied on bacteria by Baptista et al.[32] and using MetaboAnalyst 4.0[33] for metabolite comparative quantification and annotation. Flow infusion electrospray ionization high resolution mass spectrometry (FIE-HRMS) was used to profile extracted metabolites derived from treated (compound **12** vs PZQ) and control *S. mansoni* adult worms. Unsupervised principal component analysis (PCA) revealed that the metabolomics profile of worms treated with compound **12** is quite distinct from the metabolic profile of PZQ-treated and untreated worms, suggesting a different mode of action (Figure 7).

Metabolites responsible for separation between compound **12** treated and control worms (DMSO) in PCA were identified using MetaboAnalyst 4.0.[33] A total of 2123 m/z FIE-HRMS features were found to be significantly different ($p < 0.01$) between the two samples considering positive and negative ionization mode together (1210 and 913, respectively). The MetaboAnalyst 4.0-MS peaks to pathway was used to identify these variables. The software used the *mummichog* algorithm, which allows avoidance of the *a priori* identification of metabolites and the biased manual assignment of spectral features to metabolites[34] by looking for local enrichment after plotting all possible matches in the metabolic network. This method provides accurate reproduction of true activity, as the false matches distribute randomly.[34] The run analysis revealed that arachidonic acid (ARA), pentose phosphate, pyrimidine, amino sugar, and fructose and mannose metabolism were all significantly affected in compound **12** treated worms (Table 2A for significant pathways, Supplementary Data SD1 and SD2 for all identified metabolites and Supplementary Data SD3 and SD4 for all identified pathways).

Pathway identifications were performed by using MetaboAnalyst 4.0,[33] as described in the Methods section, after analysis and identification (tolerance = 3 ppm) of m/z features obtained by high resolution mass spectrometry. The tables include ranked enriched pathways, total number of hits, significant hits ($p < 0.05$), their EASE (Expression Analysis

DOI: 10.1021/acsinfecdis.9b00034
ACS Infect. Dis. XXXX, XXX, XXX−XXX

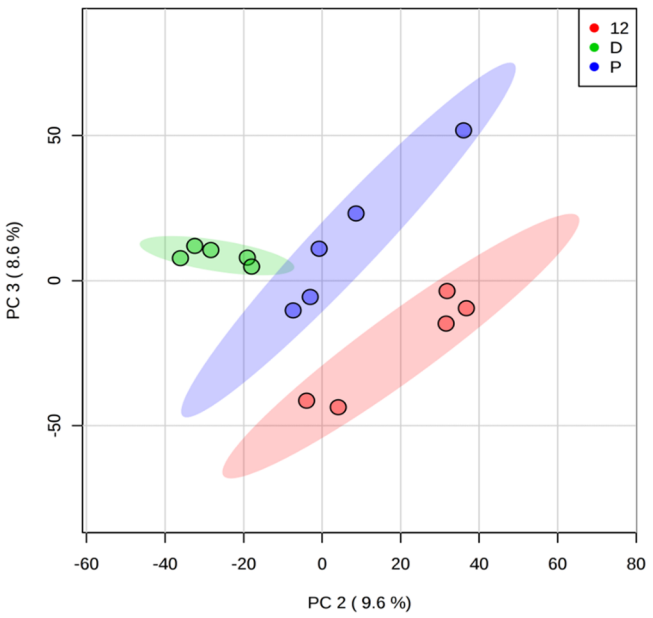

Figure 7. Principal component analysis (PCA) of *S. mansoni* adult worm metabolome. PCA score plots (positive and negative ionization mode together; colored regions display 95% confidence interval) of normalized *m/z* intensities of metabolites extracted from *S. mansoni* adult worms after 24 h of treatment with compound **12** (**12**, in red) at IC_{50} concentration (9.4 μM) compared to worms treated with DMSO (0.625%) (D, in green) and to worms treated with PZQ (P, in blue) at IC_{50} concentration (30 nM; Supporting Information, S6).

Systematic Explorer) score,[35] their raw *p*-values (Fisher's exact test, FET), and the *p*-values using a Gamma distribution.

Within the positive ionization mode, the only pathway found to be significantly affected by compound **12** was ARA metabolism. Specifically, ARA and its downstream derivatives prostaglandin (PG) E2 and/or D2 were found in higher abundance within the metabolite pool of compound **12** treated worms when compared to controls (Figure 8A). Interestingly, exogenously administered or elevated levels of host derived ARA have previously been shown to kill schistosomes *in vitro* as well as *in vivo*.[23,36] Because of this and an excellent safety profile, ARA has recently undergone clinical trials in school children within highly endemic regions.[37,38] While ARA led to worm reductions similar to PZQ in both lightly and heavily infected children, it potentiated the effect of this anthelmintic when coadministrated to both study populations. The proposed mechanism of ARA action on schistosome viability has been reported to function through activation of the tegument-associated neutral sphingomyelinase, nSMase; this enzyme is responsible for sphingomyelin hydrolysis and a consequent increase in membrane permeability and alteration of lipid balance, as well as exposure of surface antigens to antibody binding.[23,38,39] Interestingly, the reported phenotype for ARA-treated worms includes tegumental disruption and the formation of "bubble-like lesions",[23] very similar to what was observed in compound **12** treated worms. Indeed, sphingomyelin hydrolysis is associated with internal release of ceramide,[40] signaling molecules that have been previously associated with membrane blebbing and apoptosis.[41] Collectively, these observations seem to suggest that compound **12** affects schistosome survival by interfering with either ARA metabolism and/or PGE2/D2 homeostasis. Although PG-producing cyclooxygenases have not yet been identified in schistosomes,[42] prostaglandins are a major component of the schistosome lipidome[43] and are thought to be involved in host immune system evasion[44] as well as in cercarial penetration.[45] Whether these altered PGE2/PGD2 levels, induced by compound **12**, would also affect schistosome survival *in vivo* is currently unknown. However, this hypothesis seems plausible due to the importance of these downstream ARA products in modulating host interactions. Finally, and similar to the phenomenon observed for other diterpenoids on human cells,[46,47] the lipophilic structure of compound **12** may directly affect schistosome survival by altering PG and lipid balances essential for normal maintenance of the worm's heptalaminate barrier.

When examining the compound **12** induced pathways significantly enriched in the negative ionization mode, the involvement of sugar metabolism was evident. In particular, pentose phosphate pathway (PPP) metabolites were less abundant. As one of the main functions of the PPP is to generate metabolites essential for nucleic acid synthesis, it was not surprising that nucleotides and nucleotide sugars were also less abundant in compound **12** treated schistosomes. The

Table 2. Significantly Affected Pathways in Adult *S. mansoni* Worms after 24 h of Treatment with Compound 12 and PZQ (Compared to DMSO Control Worms)

	A. Compound **12** vs Control Worms					
	pathway total	hits tot.	hits sig.	EASE	FET	Gamma
arachidonic acid metabolism[a]	14	6	6	0.10996	0.01598	0.00013
pentose phosphate pathway[b]	19	12	11	0.03670	0.00711	0.00008
pyrimidine metabolism[b]	32	17	14	0.05077	0.01550	0.00009
amino sugar and nucleotide sugar[b] metabolism	27	14	12	0.05509	0.01460	0.00009
fructose and mannose metabolism[b]	16	10	9	0.09049	0.02083	0.00012
	B. PZQ vs Control Worms					
	pathway total	hits tot.	hits sig.	EASE	FET	Gamma
glycolysis or gluconeogenesis[b]	25	15	14	0.039364	0.00830	0.00008
citrate cycle (TCA cycle)[b]	20	10	10	0.061894	0.00890	0.00010
fructose and mannose metabolism[b]	16	10	10	0.061894	0.00890	0.00010
pentose and glucuronate interconversions[b]	11	9	9	0.09122	0.01435	0.00012
pentose phosphate pathway[b]	19	12	11	0.11081	0.02864	0.00013
alanine, aspartate, and glutamate metabolism[b]	17	12	11	0.11081	0.02864	0.00013

[a]From metabolites identified in positive ionization mode. [b]From metabolites identified in negative ionization mode.

DOI: 10.1021/acsinfecdis.9b00034
ACS Infect. Dis. XXXX, XXX, XXX−XXX

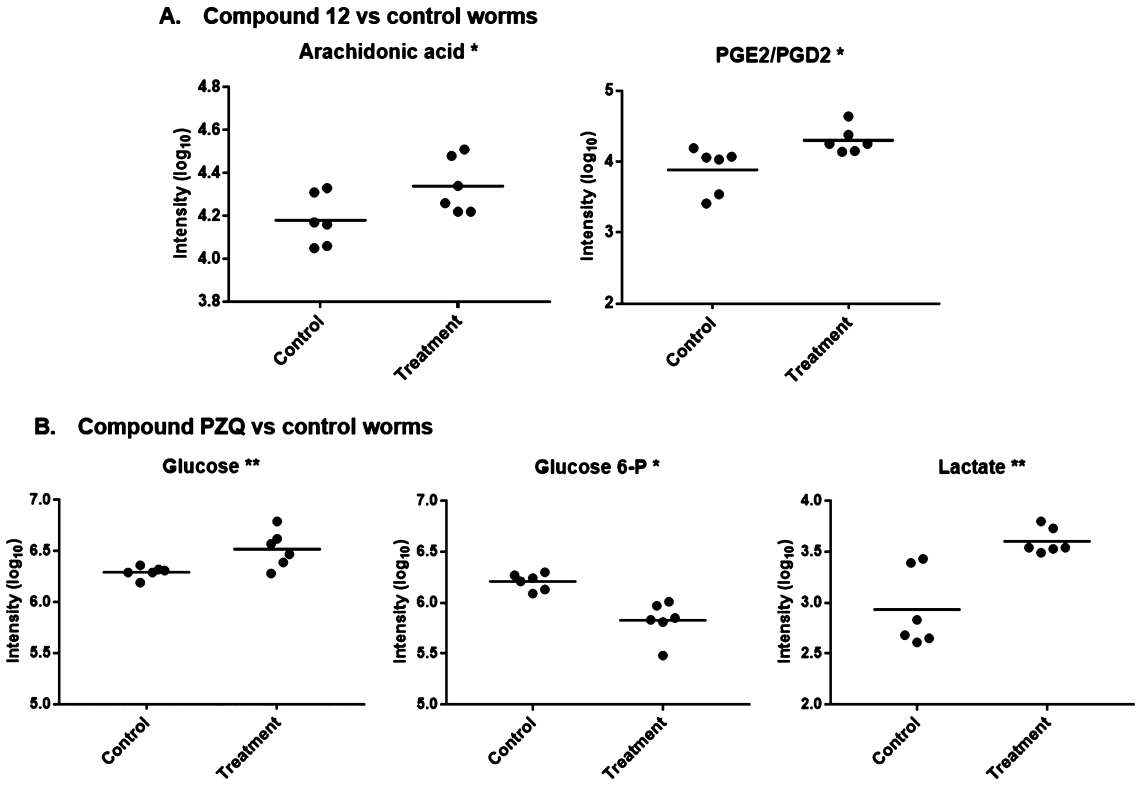

Figure 8. Significant affected key metabolites found in treated schistosomes. Some key metabolites with significantly (*$p < 0.01$, **$p < 0.001$) different concentrations found between control and treatment. (A) Compound **12** treatment induces increased production of arachidonic acid and prostaglandins (e.g., PGE2 or PGD2 level; as the two prostaglandins are structural isomers with the same exact mass and belonging to the same enriched pathway, the algorithm is not able to distinguish between them). (B) PZQ-treatment induces increased production of glucose and lactate, while levels of glucose 6-phosphate were decreased.

other main function of the PPP is in the synthesis of NADPH that, in mammals, is necessary for fatty acid synthesis; therefore, the PPP would be downregulated when fatty acids are in abundance. Despite the lack of a proper *de novo* lipogenesis, schistosomes can synthesize new fatty acids by modification of host-derived ones using NADPH-dependent enzymes;[48] therefore, similar to mammals, we speculate that the PPP was likely downregulated in compound **12** treated worms due to the increase in abundance of fatty acids (here ARA).

To determine if these metabolomics changes are specific to compound **12** or are generally induced in schistosomes upon all anthelmintic stresses, interrogation of the metabolomics signatures between PZQ-treated and untreated worms was subsequently performed. To our knowledge, this has not been done before and may also represent a novel way of identifying PZQ's mechanism of action. A total of 2756 m/z HRMS features were found to be significantly different ($p < 0.01$) between the two samples considering positive and negative ionization modes together (1725 and 1031, respectively). Affected pathways mainly belonged to sugar metabolism (i.e., glycolysis or gluconeogenesis), citrate cycle, fructose and mannose metabolism, pentose and glucuronate interconversions, PPP, and the metabolism of the glucogenic amino acids alanine, aspartate, and glutamate (see Table 2B for significant pathways, Supplementary Data SD1 and SD2 for all identified metabolites, and Supplementary Data SD5 and SD6 for all identified pathways). In particular, the main product of schistosome carbohydrate metabolism, lactate, was found to be more abundant than in the control; other glucose pool metabolites (e.g., glucose 6-P) were found in decreased abundances, while glucose itself was found to be in much higher concentration (Figure 8B). Considering the recent report describing PZQ as a human serotonin 5-HT_{2b} receptor agonist,[24] we assessed how our metabolomics data paralleled serotonin pathway activation. In schistosomes, serotonin increases carbohydrate catabolism by increasing glycogen utilization, stimulating glycolysis and, therefore, increasing production of lactate.[49] Moreover, serotonin also causes an increase in glucose uptake.[49] Disturbance of carbohydrate metabolism, with an increase in glycogen breakdown, and an impairment of serotonin stimulation of carbohydrate metabolism have also been described in PZQ-treated schistosomes.[25] All these previously reported effects are compatible with the observed data, supporting the idea that PZQ could alter serotonin signaling in schistosomes too. A different hypothesis that could justify an increased glucose concentration, associated with a decreased concentration of glucose-6-phosphate, is a direct interference of PZQ in the glycolytic pathway. In schistosomes, the enzyme responsible for glucose phosphorylation is a hexokinase with an intermediate characteristic between mammalian hexokinase and glucokinase and is a strong point of glycolysis regulation.[50] An antagonist effect of PZQ on hexokinase was recently demonstrated on the trematode *Clonorchis sinensis*,[26] whose hexokinase share 69% identity with *S. mansoni*. A similar antagonist action of PZQ on *S. mansoni* hexokinase would justify a decreased glucose phosphorylation. However, we cannot exclude that the observed effects on glycolysis could also be a consequence of generalized cellular stress.

DOI: 10.1021/acsinfecdis.9b00034
ACS Infect. Dis. XXXX, XXX, XXX−XXX

CONCLUSIONS

In summary, we demonstrated that sclareol, a nontoxic diterpenoid widely used in the cosmetic and food industries, has antischistosomal properties. By pursuing the medicinal chemistry development of 14 derivatives, we have created more active compounds. The most potent derivative, compound **12**, showed a selective improved potency on larval schistosomes ($IC_{50} \approx 2.2$ μM, SI ≈ 22 when compared to HepG2 cells), juveniles ($IC_{50} = 1.1$ μM, SI = 44.5), and adult worms ($IC_{50} = 9.4$ μM, SI = 5.2). Moreover, phenotypic analyses by SEM and metabolomics investigation revealed that this diterpenoid likely acts by disrupting surface membranes through alterations of ARA metabolism. This mechanism of action is quite distinct from that ascertained by metabolomics-based investigation of PZQ-treated worms, which revealed carbohydrate metabolism alterations similar to that observed upon serotonin signaling. Further mechanistic analyses of sclareol derivatives could provide important information for the development of novel antischistosomal molecules.

METHODS

Chemistry. Enantiomerically pure (−)-sclareol was purchased from Sigma-Aldrich (357995-1G, CAS 515-03-7) and used without further purification. The diterpenoid small collection was obtained by PhytoQuest Ltd., and all other reagents or solvents were obtained from Sigma-Aldrich or Fisher Scientific and used without purification. The synthesized sclareol derivatives were characterized by high resolution mass spectrometry (HRMS) and ^{1}H, ^{13}C, and two-dimensional nuclear magnetic resonance (NMR) spectroscopy (2D COSY, HSQC). NMR spectra were recorded on a Bruker Avance 500 MHz NMR spectrometer, with $CDCl_3$ used as solvent and NMR spectra referenced to the $CDCl_3$ residual peak. All the reactions were checked by thin layer chromatography (TLC) on precoated TLC aluminum sheets of silica gel. All the synthesized derivatives were purified by column chromatography on silica gel (35−70 mesh) using the eluents indicated. Mass spectrometry was performed on an Orbitrap Fusion Thermo Scientific with a Dionex UltiMate 3000 UHPLC system. Microwave-assisted reactions were performed in a CEM discover microwave synthesizer 2005 (908010, serial number DU9667).

The general methods for synthesis and the characterization (^{1}H and ^{13}C NMR, HRMS) of all the synthesized compounds as well as ^{1}H and ^{13}C NMR spectra of key compounds (**7**, **8**, **11**, **12**, and **14**) can be found in the Supporting Information.

Compound Handling and Storage. (−)-Sclareol and all the synthesized derivatives were solubilized in DMSO (Fisher Scientific, Loughborough, UK) and stored at −20 °C at a stock concentration of 16 mM.

***Schistosoma mansoni* Schistosomula Culture and Compound Screening.** *S. mansoni* (Puerto Rican Strain, Naval Medical Research Institute, NMRI) schistosomula were obtained by mechanical transformation[51] of *S. mansoni* cercariae collected after exposure of infected *Biomphalaria glabrata* (NMRI) snails to 2 h of light at 26 °C. Newly transformed schistosomula were deposited in 384-well black-sided microtiter plates (PerkinElmer, MA, USA) and screened by the high throughput screening platform Roboworm as previously described[18,27] with a final DMSO concentration of 0.625%. The effect of compounds on phenotype and motility of schistosomula was analyzed after 72 h using the image analysis model described by Paveley et al.[52] Phenotype and motility scores were used to calculate IC_{50} values derived from dose response titrations (50, 25, 10, and 1 μM) by using GraphPad Prism 7.02.

***Schistosoma mansoni* Juvenile Worm Culture and Compound Screening.** *S. mansoni* juvenile worms were recovered from hepatic portal veins by perfusion[53] 3 weeks after percutaneous exposure of TO mice (Harlan, UK) to ∼4000 *S. mansoni* cercariae and collected as previously described.[18] Briefly, collected worms were transferred into 50 mL falcon tubes and subjected to three series of centrifugation (300*g* for 2 min) and washing (in phenol-red free DMEM) steps with the final washed parasites pelleted by gravity. Between 10 and 15 juvenile worms were cultured per well in a 96-well tissue culture plate (Fisher Scientific, Loughborough, UK). Each well contained 200 μL of modified DMEM (Gibco, Paisley, UK) supplemented with 10% v/v HEPES (Sigma-Aldrich, Gillingham, UK), 10% v/v fetal calf serum (Gibco, Paisley, UK), 0.7% v/v 200 mM L-glutamine (Gibco, Paisley, UK), and 1% v/v antibiotic/antimycotic (Gibco, Paisley, UK). After incubation for 2 h at 37 °C in a humidified atmosphere containing 5% CO_2, test compounds were added to obtain the final concentrations of 50, 25, 12.5, 6.25, 3.13, 1.65, and 0.8 μM (0.3% DMSO final concentration). After 72 h, worms were scored manually using microscopic methods previously described.[18] Briefly, a score of 0 equaled no detectable movement, 1 included movement of the suckers and/or slight body contraction, 2 represented slow movement of anterior and posterior regions, 3 equated to sluggish movement of the full body, and 4 represented normal movement. IC_{50} values were determined using GraphPad Prism 7.02.

***Schistosoma mansoni* Adult Worm Culture and Compound Screening.** Mature adult parasites were recovered from hepatic portal veins by perfusion[53] 7 weeks after percutaneous exposure of TO mice (Harlan, UK) to 180 *S. mansoni* cercariae. Three adult worm pairs were cultured per well in a 48-well tissue culture plate (Fisher Scientific, Loughborough, UK). Each well included 1 mL of modified DMEM (Gibco, Paisley, UK) media containing 10% v/v Hepes (Sigma-Aldrich, Gillingham, UK), 10% v/v Foetal Calf Serum (Gibco, Paisley, UK), 0.7% v/v 200 mM L-Glutamine (Gibco, Paisley, UK), 1% v/v Antibiotic/antimycotic (Gibco, Paisley, UK). After incubation for 2 h at 37 °C in a humidified atmosphere containing 5% CO_2, test compounds were added to obtain the final concentrations of 50, 25, 12.5, 6.25, and 3.13 μM (0.3% DMSO final concentration). After 72 h, worms were scored manually using microscopic methods described in the literature[54] and eggs collected and counted from each well. IC_{50} values were determined using GraphPad Prism 7.02.

HepG2 Cell Culture and MTT Assay. HepG2 human liver cancer cells were grown to ∼80% confluency in a modified BME culture media (containing 10% v/v fetal bovine serum, 1% v/v MEM nonessential amino acid solution, 1% v/v 200 mM L-glutamine, and 1% v/v antibiotic/antimycotic). Confluent cells were subjected to cytotoxicity assays as previously described.[18,27] Briefly, 2.5×10^4 cells per well were cultured in a black walled 96-well microtiter plate (Fisher Scientific, Loughborough, UK) and incubated for 24 h at 37 °C in a humidified atmosphere with 5% CO_2. Test compounds were then titrated from 100 to 3.13 μM (1.25 final % DMSO), and negative (DMSO; 1.25%) and positive (1% v/v Triton X-100)[55] controls were included. After 24 h of incubation, the

DOI: 10.1021/acsinfecdis.9b00034
ACS Infect. Dis. XXXX, XXX, XXX−XXX

MTT assay was performed as described.[18,27] CC_{50} values were determined using GraphPad Prism 7.02.

Scanning Electron Microscopy (SEM). Adult worms, cultured for 72 h with sublethal concentrations of test compounds and negative (DMSO) controls, were collected and prepared for SEM analysis. Several steps from Collins et al.[56] were adapted as previously described.[18] Briefly, collected schistosomes were relaxed in 1 mL of anesthetic (1% ethyl 3-aminobenzoate methane (Sigma-Aldrich, Gillingham, UK) dissolved in DMEM) and then killed in 1 mL of 0.6 mM $MgCl_2$ (Fisher Scientific, Loughborough, UK). After washing in PBS, worms were placed in SEM fixative (0.1 M sodium cacodylate, 2.5% v/v glutaraldehyde (Agar Scientific, Stansted, UK) in ultrapure water) and stored at 4 °C until ready for SEM analysis. In preparation for SEM analysis, the stored samples were exposed to a number of wash, staining, and dehydration steps as described[18] and finally mounted for imaging. SEM analysis was conducted using a Hitachi S-4700 FESEM microscope (Ultra High Resolution, an accelerating voltage of 5.0 kV with a working distance of 5.0 mm). Images were captured at 2560 × 1920 resolution.

Metabolomics Sample Preparation and Metabolite Extraction. The procedure previously described by Baptista et al.[32] was adapted to schistosome materials. Adult male worms were collected and cultured in media as described in previous paragraphs. In brief, 24-well plates were set up with 10 male worms per well (one biological replicate) for a total of 18 wells (6 replicates per 3 time points) per treatment (compound **12** and PZQ, at their respective IC_{50} values, 9.4 μM and 30 nM, and control). At each time point (0, 12, 24 h), worms were removed from culture, immersed in liquid nitrogen to quench metabolism, and stored at −80 °C. In preparation for the extraction, samples were thawed, centrifuged (10 °C, 2000 rpm), and washed with phosphate buffer saline. Worms were disrupted by a mill bead homogenizer, and extraction was performed in a chloroform/methanol/water 2:5:2 solution. After a final centrifugation, 100 μL of solution was transferred in mass vials for FIE-HRMS analysis.

Metabolomics Analysis. Extracted metabolites were analyzed by flow infusion electrospray ionization high-resolution mass spectrometry (FIE-HRMS) in the High Resolution Metabolomics Laboratory (HRML), Aberystwyth University. FIE-HRMS was performed by a Q-Exactive Plus mass analyzer equipped with an UltiMate 3000 UHPLC system, which includes a Thermo-Scientific binary pump, column compartment (not used), and auto sampler. Metabolite fingerprints were created in both positive and negative polarity switching mode. Ion intensities were acquired between m/z 55 and 1200 for 3.5 min in profiling mode at a resolution setting of 280,000. Twenty μL of each extracts was injected by an autosampler into a flow of 100 $\mu L \cdot min^{-1}$ methanol/water (70:30, v/v). Electrospray ionization (ESI) source parameters were set in agreement with manufacturer's recommendations. An in-house data aligning routine in Matlab (R2013b, The MathWorks) was used to join mass spectra around the apex of the infusion maximum into a single mean intensity matrix (runs × m/z) for each ionization mode. Data from the matrix were log_{10}-transformed and used for statistical analysis performed by MetaboAnalyst 4.0.-Statistical analysis.[33] Metabolites and pathway identification were performed by the MetaboAnalyst 4.0.-MS peaks to pathway[33] (tolerance = 3 ppm, model organism = *S. mansoni*; time point = 24 h, as this had the highest number of significantly different features). MetaboAnalyst identified pathways on the basis of the *mummichog* algorithm, which predicts metabolome changes directly from mass spectrometry data, without the *a priori* identification of metabolites and avoiding the biased manual assignment of spectral features to metabolites.[34] *Mummichog* looks for local enrichment after plotting all possible matches in the metabolic network, providing accurate reproduction of true activity, as the false matches will distribute randomly.[34] Examples of key metabolites were analyzed for the significant difference (t test) between control and treatment on Microsoft Excel and by GraphPad Prism 7.02.

Ethics Statement. All procedures performed on mice adhered to the United Kingdom Home Office Animals (Scientific Procedures) Act of 1986 (project license PPL 40/3700) as well as the European Union Animals Directive 2010/63/EU and were approved by Aberystwyth University's (AU) Animal Welfare and Ethical Review Body (AWERB).

■ ASSOCIATED CONTENT

Supporting Information

The Supporting Information is available free of charge on the ACS Publications website at DOI: 10.1021/acsinfecdis.9b00034.

Identification (matched compounds as KEGG code) of metabolites found by positive ionization mode (XLSX)

Identification (matched compounds as KEGG code) of metabolites found by negative ionization mode (XLSX)

Ranked enriched pathways with the total number of hits found by positive ionization mode after compound **12** treatment, significant hits ($p < 0.05$), their EASE (Expression Analysis Systematic Explorer) score,[35] their raw p-values (Fisher's Exact Test, FET), and the p-values using a Gamma distribution (XLSX)

Ranked enriched pathways with the total number of hits found by negative ionization mode after compound **12** treatment, significant hits ($p < 0.05$), their EASE (Expression Analysis Systematic Explorer) score,[35] their raw p-values (Fisher's Exact Test, FET), and the p-values using a Gamma distribution (XLSX)

Ranked enriched pathways with the total number of hits found by positive ionization mode after PZQ treatment, significant hits ($p < 0.05$), their EASE (Expression Analysis Systematic Explorer) score,[35] their raw p-values (Fisher's Exact Test, FET), and the p-values using a Gamma distribution (XLSX)

Ranked enriched pathways with the total number of hits found by negative ionization mode after PZQ treatment, significant hits ($p < 0.05$), their EASE (Expression Analysis Systematic Explorer) score,[35] their raw p-values (Fisher's Exact Test, FET), and the p-values using a Gamma distribution (XLSX)

General methods for synthesis and characterization (^{1}H NMR and ^{13}C NMR peak lists, HRMS) of all the synthesized compounds, ^{1}H NMR and ^{13}C NMR spectra of key compounds, screening of diterpenoid small collection on *S. mansoni* schistosomula, antischistosomal and cytotoxicity data summary (IC_{50} and CC_{50} with 95% confidence interval), scatter graphs for *S. mansoni* juvenile, adult worms and eggs count after treatments with key compounds, and PZQ titration on adult worms (PDF)

DOI: 10.1021/acsinfecdis.9b00034
ACS Infect. Dis. XXXX, XXX, XXX−XXX

AUTHOR INFORMATION

Corresponding Authors

*E-mail: krh@aber.ac.uk (K.F.H.).
*E-mail: WestwellA@cf.ac.uk (A.D.W.).

ORCID

Karl F. Hoffmann: 0000-0002-3932-5502

Author Contributions

A.C., A.D.W., and K.F.H. conceived and designed the experiments. A.C. performed compound synthesis and characterization and *S. mansoni* and HepG2 cell screening; R.J.N. provided plant-derived diterpenoids, and H.W. performed the plant-derived diterpenoid screening. A.C., R.B., J.E.F.-T., M.B., and L.A.J.M. performed metabolomics. A.C. prepared the original draft of the manuscript, and A.D.W. and K.F.H. edited and revised it.

Notes

The authors declare no competing financial interest.

ACKNOWLEDGMENTS

We thank the Welsh Government, Life Sciences Research Network Wales scheme for financial support to A.C. and R.B. IBERS receives strategic funding from the BBSRC. We thank all of Prof. Karl F. Hoffmann's laboratory for help in maintaining the *S. mansoni* life cycle. We thank Prof. Andrea Brancale for the use of the microwave synthesiser.

REFERENCES

(1) Caniard, A., Zerbe, P., Legrand, S., Cohade, A., Valot, N., et al. (2012) Discovery and functional characterization of two diterpene synthases for sclareol biosynthesis in *Salvia sclarea* (L.) and their relevance for perfume manufacture. *BMC Plant Biol. 12* (1), 119.

(2) Smith, R. L., Waddell, W. J., Cohen, S. M., Feron, V. J., Marnett, L. J., Portoghese, P. S., Rietjens, I. M. C. M., Adams, T. B., Gavin, C. L., Mcgowen, M. M., Taylor, S. V., and Williams, M. C. (2009) GRAS 24: the 24th publication by the FEMA Expert Panel presents safety and usage data on 236 new generally recognized as safe flavoring ingredients. *Food Technol. 63* (6), 46−105.

(3) The RIFM EXPERT Panel, Belsito, D., Bickers, D., Bruze, M., Calow, P., Greim, H., Hanifin, J. M., Rogers, A. E., Saurat, J. H., Sipes, I. G., and Tagami, H. (2008) A toxicologic and dermatologic assessment of cyclic and non-cyclic terpene alcohols when used as fragrance ingredients. *Food Chem. Toxicol. 46*, S1−S71.

(4) Sirikantaramas, S., Yamazaki, M., and Saito, K. (2008) Mechanisms of resistance to self-produced toxic secondary metabolites in plants. *Phytochem. Rev. 7*, 467−477.

(5) Tapia, L., Torres, J., Mendoza, L., Urzua, A., Ferreira, J., Pavani, M., and Wilkens, M. (2004) Effect of 13- epi -sclareol on the bacterial respiratory chain. *Planta Med. 70*, 1058−1063.

(6) Ma, M., Feng, J., Li, R., Chen, S., and Xu, H. (2015) Synthesis and antifungal activity of ethers, alcohols, and iodohydrin derivatives of sclareol against phytopathogenic fungi *in vitro*. *Bioorg. Med. Chem. Lett. 25* (14), 2773−7.

(7) Zhang, T., Wang, T., and Cai, P. (2017) Sclareol inhibits cell proliferation and sensitizes cells to the antiproliferative effect of bortezomib via upregulating the tumor suppressor caveolin-1 in cervical cancer cells. *Mol. Med. Rep. 15*, 3566−74.

(8) Wang, L., He, H. S., Yu, H. L., Zeng, Y., Han, H., He, N., et al. (2015) Sclareol, a plant diterpene, exhibits potent antiproliferative effects via the induction of apoptosis and mitochondrial membrane potential loss in osteosarcoma cancer cells. *Mol. Med. Rep. 11*, 4273−4278.

(9) Noori, S., Hassan, Z. M., and Salehian, O. (2013) Sclareol Reduces CD4 + CD25 + FoxP3 + T-reg cells in a breast cancer model in vivo. *Iran J. Immunol. 10* (March), 10−21.

(10) Dimas, K., Papadaki, M., Tsimplouli, C., Hatziantoniou, S., Alevizopoulos, K., et al. (2006) Labd-14-ene-8,13-diol (sclareol) induces cycle arrest and apoptosis in human breast cancer cells and enhances the activity of anticancer drugs. *Biomed. Pharmacother. 60*, 127−133.

(11) El Ridi, R. A. F., and Tallima, H. A. M. (2013) Novel therapeutic and prevention approaches for schistosomiasis: review. *J. Adv. Res. 4* (5), 467−78.

(12) CDC. *Neglected Tropical Diseases*, https://www.cdc.gov/globalhealth/ntd/.

(13) Vale, N., Gouveia, M. J., Rinaldi, G., Brindley, P. J., Gartner, F., and da Costa, J. M. C. (2017) Praziquantel for schistosomiasis: single-drug metabolism revisited, mode of action, and resistance. *Antimicrob. Agents Chemother. 61* (5), 1−16.

(14) Doenhoff, M. J., Cioli, D., and Utzinger, J. (2008) Praziquantel: mechanisms of action, resistance and new derivatives for schistosomiasis. *Curr. Opin. Infect. Dis. 21* (6), 659−67.

(15) Barros de Alencar, M. V. O., de Castro e Sousa, J. M., Rolim, H. M. L., de Medeiros, M. G. F., Cerqueira, G. S., de Castro Almeida, F. A., Citó, A. M. G. L., Ferreira, P. M. P., Lopes, J. A. D., et al. (2017) Diterpenes as lead molecules against neglected tropical diseases. *Phyther Res. 31*, 175−201.

(16) Neves, B., Andrade, C., and Cravo, P. (2015) Natural products as leads in schistosome drug discovery. *Molecules 20*, 1872−903.

(17) de Moraes, J. (2015) Natural products with antischistosomal activity. *Future Med. Chem. 7* (6), 801−20.

(18) Crusco, A., Bordoni, C., Chakroborty, A., Whatley, K. C. L., Whiteland, H., Westwell, A. D., and Hoffmann, K. F. (2018) Design, synthesis and anthelmintic activity of 7-keto-sempervirol analogues. *Eur. J. Med. Chem. 152*, 87−100.

(19) Edwards, J., Brown, M., Peak, E., Bartholomew, B., Nash, R. J., and Hoffmann, K. F. (2015) The diterpenoid 7-keto-sempervirol, derived from *Lycium chinense*, displays anthelmintic activity against both *Schistosoma mansoni* and *Fasciola hepatica*. *PLoS Negl Trop Dis. 9* (3), e0003604.

(20) Shakeel-U-Rehman, Rah, B., Lone, S. H., Rasool, R. U., Farooq, S., Nayak, D., Chikan, N. A., Chakraborty, S., Behl, A., Mondhe, D. M., Goswami, A., and Bhat, K. A. (2015) Design and synthesis of antitumor heck-coupled sclareol analogues: Modulation of BH3 family members by SS-12 in autophagy and apoptotic cell death. *J. Med. Chem. 58* (8), 3432−3444.

(21) O'Boyle, N. M., Bostrom, J., Sayle, R. A., and Gill, A. (2014) Using matched molecular series as a predictive tool to optimize biological activity. *J. Med. Chem. 57*, 2704−2713.

(22) Topliss, J. G. (1977) A manual method for applying the Hansch approach to drug design. *J. Med. Chem. 20* (4), 463−9.

(23) El Ridi, R., Aboueldahab, M., Tallima, H., Salah, M., Mahana, N., Fawzi, S., Mohamed, S. H., and Fahmy, O. M. (2010) *In vitro* and *in vivo* activities of arachidonic acid against *Schistosoma mansoni* and *Schistosoma haematobium*. *Antimicrob. Agents Chemother. 54* (8), 3383−3389.

(24) Chan, J. D., Cupit, P. M., Gunaratne, G. S., Mccorvy, J. D., Yang, Y., Stoltz, K., Webb, T. R., Dosa, P. I., Roth, B. L., Abagyan, R., Cunningham, C., and Marchant, J. S. (2017) The anthelmintic praziquantel is a human serotoninergic G-protein-coupled receptor ligand. *Nat. Commun. 8* (1910), 1−7.

(25) Harder, A., Abbink, J., Andrews, P., and Thomas, H. (1987) Praziquantel impairs the ability of exogenous serotonin to stimulate carbohydrate metabolism in intact *Schistosoma mansoni*. *Z. Parasitenkd. 73*, 442−5.

(26) Chen, T., Ning, D., Sun, H., Li, R., Shang, M., Li, X., Wang, X., Chen, W., Liang, C., Li, W., Mao, Q., Li, Y., Deng, C., and Wang, L. (2014) Sequence analysis and molecular characterization of *Clonorchis sinensis* hexokinase, an unusual trimeric 50- kDa glucose-6-phosphate-sensitive allosteric enzyme. *PLoS One. 9* (9), e107940.

(27) Nur-e-alam, M., Yousaf, M., Ahmed, S., Al-sheddi, E. S., Parveen, I., Fazakerley, D. M., Bari, A., Ghabbour, H. A., Threadgill, M. D., Whatley, K. C. L., Hoffmann, K. F., and Al-rehaily, A. J. (2017)

DOI: 10.1021/acsinfecdis.9b00034
ACS Infect. Dis. XXXX, XXX, XXX−XXX

Neoclerodane diterpenoids from *Reehal fatima, Teucrium yemense*. *J. Nat. Prod. 80*, 1900−8.
(28) Zhang, J., Chung, T. D. Y., and Oldenburg, K. R. (1999) A simple statistical parameter for use in evaluation and validation of high throughput screening assays. *J. Biomol Screen. 4* (2), 67−73.
(29) Hua, S. K., Wang, J., Chen, X. B., Xu, Z. Y., and Zeng, B. B. (2011) Scalable synthesis of methyl ent-isocopalate and its derivatives. *Tetrahedron 67* (6), 1142−4.
(30) Rogachev, V., Löhl, T., Markert, T., and Metz, P. (2011) A short and efficient synthesis of (+) -totarol. *ARKIVOC 2012*, 172−180.
(31) Mafud, A. C., Silva, M. P. N., Monteiro, D. C., Oliveira, M. F., Resende, J. G., Coelho, M. L., de Sousa, D. P., Mendonça, R. Z., Pinto, P. L. S., Freitas, R. M., Mascarenhas, Y. P., and de Moraes, J. (2016) Structural parameters, molecular properties, and biological evaluation of some terpenes targeting *Schistosoma mansoni* parasite. *Chem.-Biol. Interact. 244*, 129−39.
(32) Baptista, R., Fazakerley, D. M., Beckmann, M., Baillie, L., and Mur, L. A. J. (2018) Untargeted metabolomics reveals a new mode of action of pretomanid (PA-824). *Sci. Rep. 8*, 5084.
(33) Chong, J., Soufan, O., Li, C., Caraus, I., Li, S., Bourque, G., Wishart, D. S., and Xia, J. (2018) MetaboAnalyst 4.0: towards more transparent and integrative metabolomics analysis. *Nucleic Acids Res. 46* (May), W486−W494.
(34) Li, S., Park, Y., Duraisingham, S., Strobel, F. H., Khan, N., Soltow, Q. A., Jones, D. P., and Pulendran, B. (2013) Predicting network activity from high throughput metabolomics. *PLoS Comput. Biol. 9* (7), e1003123.
(35) Hosack, D. A., Dennis, G., Jr., Sherman, B. T., Lane, H. C., and Lempicki, R. A. (2003) Identifying biological themes within lists of genes with EASE. *Genome Biol. 4* (10), R70.
(36) Hanna, V. S., Gawish, A., El-Dahab, M. A., Tallima, H., and El Ridi, R. (2018) Is arachidonic acid an endoschistosomicide ? *J. Adv. Res. 11*, 81−89.
(37) Barakat, R., El-Ela, N. E. A., Sharaf, S., El Sagheer, O., Selim, S., Tallima, H., Bruins, M. J., Hadley, K. B., and El Ridi, R. (2015) Efficacy and safety of arachidonic acid for treatment of school-age children in *Schistosoma mansoni* high-endemicity regions. *Am. J. Trop. Med. Hyg. 92* (4), 797−804.
(38) El Ridi, R., Tallima, H., and Migliardo, F. (2017) Biochemical and biophysical methodologies open the road for effective schistosomiasis therapy and vaccination. *Biochim. Biophys. Acta, Gen. Subj. 1861* (1), 3613−20.
(39) Tallima, H., Salah, M., and El Ridi, R. (2005) *In vitro* and *in vivo* effects of unsaturated fatty acids on *Schistosoma mansoni* and *S. haematobium* lung-stage larvae. *J. Parasitol. 91* (5), 1094−1102.
(40) Redman, C. A., Kennington, S., Spathopoulou, T., and Kusel, J. R. (1997) Interconversion of sphingomyelin and ceramide in adult *Schistosoma mansoni*. *Mol. Biochem. Parasitol. 90*, 145−53.
(41) Sillence, D. J. (2001) Apoptosis and signalling in acid sphingomyelinase deficient cells. *BMC Cell Biol. 2*, 24.
(42) Howe, K. L., Bolt, B. J., Shafie, M., Kersey, P., and Berriman, M. (2017) WormBase ParaSite − a comprehensive resource for helminth genomics. *Mol. Biochem. Parasitol. 215*, 2−10.
(43) Giera, M., Kaisar, M. M. M., Derks, R. J. E., Steenvoorden, E., Kruize, Y. C. M., Hokke, C. H., Yazdanbakhsh, M., and Everts, B. (2018) The *Schistosoma mansoni* lipidome: leads for immunomodulation. *Anal. Chim. Acta 1037*, 107−18.
(44) Salafsky, B., and Fusco, A. C. (1987) *Schistosoma mansoni*: A comparison of secreted vs nonsecreted eicosanoids in developing schistosomulae and adults. *Exp. Parasitol. 64*, 361−7.
(45) Salafsky, A. B., Wang, Y., Kevin, M. B., Hill, H., and Fusco, A. C. (1984) The role of prostaglandins in cercarial (*Schistosoma mansoni*) response to free fatty acids. *J. Parasitol. 70* (4), 584−591.
(46) Hiruma-Lima, C. A., Gracioso, J. S., Toma, W., Almeida, A. B., Paula, A. C. B., Brasil, D. S. B., et al. (2001) Gastroprotective effect of aparisthman, a diterpene isolated from *Aparisthmium cordatum*, on experimental gastric ulcer models in rats and mice. *Phytomedicine 8* (2), 94−100.
(47) Parra, T., Benites, J., Ruiz, L. M., Sepulveda, B., Simirgiotis, M., and Areche, C. (2015) Gastroprotective activity of ent -beyerene derivatives in mice: effects on gastric secretion, endogenous prostaglandins and non-protein sulfhydryls. *Bioorg. Med. Chem. Lett. 25* (14), 2813−7.
(48) Brouwers, J. F. H. M., Smeenk, I. M. B., van Golde, L. M. G., and Tielens, A. G. M. (1997) The incorporation, modification and turnover of fatty acids in adult *Schistosoma mansoni*. *Mol. Biochem. Parasitol. 88*, 175−185.
(49) Rahman, M. S., Mettrick, D. F., and Podesta, R. B. (1985) *Schistosoma mansoni*: effects of in vitro serotonin (5-HT) on aerobic and anaerobic carbohydrate metabolism. *Exp. Parasitol. 60*, 10−17.
(50) Tielens, A. G., van den Heuvel, J. M., van Mazijk, H. J., Wilson, J. E., and Shoemaker, C. B. (1994) The 50-kDa glucose 6-phosphate-sensitive hexokinase of *Schistosoma mansoni*. *J. Biol. Chem. 269* (40), 24736−24741.
(51) Colley, D. G., and Wikel, S. K. (1974) *Schistosoma mansoni*: simplified method for the production of schistosomules. *Exp. Parasitol. 35* (1), 44−51.
(52) Paveley, R. A., Mansour, N. R., Hallyburton, I., Bleicher, L. S., Benn, A. E., Mikic, I., Guidi, A., Gilbert, I. H., Hopkins, A. L., and Bickle, Q. D. (2012) Whole organism high-content screening by label-free, image-based bayesian classification for parasitic diseases. *PLoS Neglected Trop. Dis. 6* (7), e1762.
(53) Smithers, S., and Terry, R. (1965) The infection of laboratory hosts with cercariae of *Schistosoma mansoni* and the recovery of the adult worms. *Parasitology 55* (4), 695−700.
(54) Ramirez, B., Bickle, Q., Yousif, F., Fakorede, F., Mouries, M., and Nwaka, S. (2007) Schistosomes: challenges in compound screening. *Expert Opin. Drug Discovery 2* (Suppl. 1), S53−62.
(55) Dayeh, V. R., Chow, S. L., Schirmer, K., Lynn, D. H., and Bols, N. C. (2004) Evaluating the toxicity of Triton X-100 to protozoan, fish, and mammalian cells using fluorescent dyes as indicators of cell viability. *Ecotoxicol. Environ. Saf. 57*, 375−82.
(56) Collins, J. J., Wang, B., Lambrus, B. G., Tharp, M. E., Iyer, H., and Newmark, P. A. (2013) Adult somatic stem cells in the human parasite *Schistosoma mansoni*. *Nature 494* (7438), 476−9.

DOI: 10.1021/acsinfecdis.9b00034
ACS Infect. Dis. XXXX, XXX, XXX−XXX